Dynamic Loads in Parallel Shaft Transmissions Part 1

Hsiang-Hsi (Edward) Lin
Memphis State University, Memphis, TN

Ronald L. Huston
University of Cincinnati, Cincinnati, OH

John J. Coy
NASA Lewis Research Center, Cleveland, OH

Introduction

Recently, there has been increased interest in the dynamic effects in gear systems. This interest is stimulated by demands for stronger, higher speed, improved performance, and longer-lived systems. This in turn has stimulated numerous research efforts directed toward understanding gear dynamic phenomena. However, many aspects of gear dynamics are still not satisfactorily understood.

For example, in industrial settings, a high performance gear system is often obtained by overdesigning and by sacrificing costs, materials, and compactness. In aerospace and military application where weight is a premium, gear systems are often designed under conditions very close to the failure limits, thereby introducing uncertainties in performance and life prediction. They are often prematurely replaced to prevent in-service failure. Moreover, gear systems are often designed by using static analyses. However, when gear systems operate at high speed, there are several factors which affect their performance. These include shaft torsional stiffness, gear tooth loading and deformation, gear tooth spacing and profile errors, rotating speeds, mounting alignment, dynamic balance of rotating elements, gear and shaft masses and inertia, and the masses and inertias of the driving (power) and driven (load) elements.

There is no agreement among researchers on the best methods for evaluating dynamic load effects. Hence, gear designers are often confronted with conflicting theories. They generally have to rely on past experience, service safety factors, and experimental data with a limited range of applicability.

The objective of this report is to provide more insight into the factors affecting dynamic loads.

Research efforts on gear system dynamics have been conducted for many years. In 1892 Lewis[1] recognized that the instantaneous tooth load was affected by the velocity of the system. In 1925, Earle Buckingham[2] headed an experimental research effort, endorsed by ASME, to measure dynamic effects. A report published in 1931 represented the first authoritative document on gear dynamics. It presented a procedure for determining the so-called dynamic load increment due to mesh dynamics and gear tooth errors.

In 1959, Attia[3] performed an experiment to determine actual instantaneous loading. He found that Buckingham's results were conservative.

In 1958, Niemann and Rettig[4] found that larger masses caused higher dynamic loads, but as the average load became larger, the effect of larger masses became less important. They also found that very heavily loaded gear systems showed no appreciable dynamic load increment, whereas in lightly and moderately loaded gear systems, there were considerable dynamic load increments. In 1958, Harris[5] suggested that for gear systems isolated from external stimuli, there are three internal sources of dynamic loads:

(1) Error in the velocity ratio measured under the working load.

(2) Parametric excitation due to stiffness variation of the gear teeth.

(3) Nonlinearity of tooth stiffness when contact is lost.

In 1970, Houser and Seireg[6] developed a generalized dynamic factor formula for spur and helical gears operating away from system resonances. The formula took into consideration the gear geometry and manufacturing parameters as well as the dynamic characteristics of the system.

In 1972, Ichimaru and Hirano[7] analyzed heavy-loaded spur gear systems with manufacturing errors under different operating conditions. They found that the change in tooth profile showed a characteristic trend to decrease dynamic load. In 1978, Cornell and Westervelt[8] presented a closed form solution for a dynamic model of a spur gear system and showed that tooth profile modification, system inertia and damping, and system critical speeds can have significant effects upon the dynamic loads. In 1981, Kasuba and Evans[9] presented a large scale digitized extended gear modeling procedure to analyze spur gear systems for both static and dynamic conditions. Their results indicated that gear mesh stiffness is probably the key element in the analysis of gear train dynamics. They showed that the gears and the adjacent drive and load systems can be designed for optimum performance in terms of minimum allowable dynamic loads for a wide range of operating speeds.

In 1981, Wang and Cheng[10] developed another dynamic load response algorithm. They reported that the dynamic load is highly dependent on the operating speed. This model is later modified by Lewicki[11] to account for the nonlinear Hertzian deformation of meshing gear teeth. The gear dynamic load found from the revised model showed little difference from the original model, since the Hertzian deflection was relatively small in comparison with the total gear tooth deflection. Nagaya and Uematsu[12] stated that because the contact point moves along the involute profile, the dynamic response should be considered as a function of both the position and speed of the moving load. In 1982, Terauchi, et al.,[13] studied the effect of tooth profile modifications on the dynamic load of spur gear systems. According to their results, the dynamic load decreased with proper profile modifications.

In this first part of the article, we present a model of a parallel shaft transmission. We consider the effects of shaft stiffness and inertia, load and power source inertias, tooth stiffness, local compliance due to contact stresses, load sharing, and friction. A parameter study is provided in the second part of the article.

AUTHORS:

DR. HSIANG HSI LIN is on the faculty at Memphis State University. His research includes kinematics, dynamics, optimization, finite element methods, and computer-aided design and analysis of mechanical systems. He received his undergraduate degree from National Chung Hsing University and did his graduate work at the University of Cincinnati.

DR. RONALD L. HUSTON is Professor of Mechanics at the University of Cincinnati and Director of the University's Institute for Applied Interdisciplinary Research. He earned his degrees in Mechanical Engineering and Engineering Mechanics from the University of Pennsylvania.

DR. JOHN J. COY is Branch Chief, Rotorcraft Systems Technology in the Propulsion Systems Division at NASA Lewis Research Center in Cleveland, OH. He took his degrees in Mechanical Engineering from the University of Cincinnati. He is the author of numerous papers and is a member of ASME. Dr. Coy is a licensed professional engineer in the State of Ohio.

Modeling

Fig. 1 depicts a model of the transmission. It consists of a motor or power source connected by a flexible shaft to the gear system. The gear system consists of a pair of involute spur gears. They are connected to the load by a second flexible shaft as shown. Symbolically, the model may be represented by a collection of masses, springs, and dampers as in Fig. 2.

Let θ_M, θ_1, θ_2, and θ_L represent the rotations of the motor, the gears, and the load. Then by using standard procedures of analysis, the governing differential equations for the rotations may be written as

$$J_M \ddot{\theta}_M + C_{s1}(\dot{\theta}_M - \dot{\theta}_1) + K_{s1}(\theta_M - \theta_1) = T_M \qquad (1)$$

$$J_1 \ddot{\theta}_1 + C_{s1}(\dot{\theta}_1 - \dot{\theta}_M) + K_{s1}(\theta_1 - \theta_M) + C_g(t)[R_{b1}\dot{\theta}_1 - R_{b2}\dot{\theta}_2] \\ + K_g(t)[R_{b1}(R_{b1}\theta_1 - R_{b2}\theta_2)] = T_{f1}(t) \qquad (2)$$

$$J_2 \ddot{\theta}_2 + C_{s2}(\dot{\theta}_2 - \dot{\theta}_1) + K_{s2}(\theta_2 - \theta_1) + C_g(t)[R_{b2}\dot{\theta}_2 - R_{b1}\dot{\theta}_1] \\ + K_g(t)[R_{b2}(R_{b2}\theta_2 - R_{b1}\theta_1)] = T_{f2}(t) \qquad (3)$$

$$J_L \ddot{\theta}_L + C_{s2}(\dot{\theta}_L - \dot{\theta}_2) + K_{s2}(\theta_L - \theta_2) = -T_L \qquad (4)$$

where J_M, J_1, J_2, and J_L represent the mass moments of inertia of the motor, the gears, and the load; C_{s1}, C_{s2}, and $C_g(t)$ are damping coefficients of the shafts and the gears; K_{s1}, K_{s2}, and $K_g(t)$ are stiffnesses of the shafts and the gears; T_M, T_L, $T_{f1}(t)$, and $T_{f2}(t)$ are motor and load torques and frictional torques on the gears; R_{b1} and R_{b2} are base circle radii of the gears; t is time; and the dots over θ indicate time differentiation.

In developing Equations 1 to 4 several simplifying assumptions are employed.

(1) The dynamic process is studied in the rotating plane of the gears. Out-of-plane twisting and misalignment are neglected.

(2) Damping due to lubrication of the gears and shafts is expressed in terms of constant damping factors.

(3) The differential equations of motion are developed by using the theoretical line of action.

(4) Low contact ratio gears are used in the analysis. Specifically, the contact ratio is taken between 1 and 2.

Analysis

A major task in the analysis is to determine the values of the stiffness, damping, and friction coefficients appearing in Equations 1 to 4. Another task is to determine the ratio of load sharing between the teeth during a mesh cycle. These factors depend on the roll angle of the gears. Thus, Equations 1 to 4 are made nonlinear by these terms.

STIFFNESS

Gear stiffness. — Consider first the stiffness coefficients K_g, K_{s1}, and K_{s2}. Let the tooth surface have the form of an involute curve. Let W_j be the transmitted load at a typical point j of the tooth profile. Let q_j be the deformation of the tooth at point j in the direction of W_j. Then the gear stiffness K_{gj} for the gear teeth in contact at j is

$$K_{gj} = \frac{W_j}{q_j} \qquad (5)$$

In general q_j will depend on the following: (1) the bending of the tooth, the shear deformation of the tooth, and the axial compression of the tooth; (2) the deflection due to the flexibility of the tooth foundation and fillet; and (3) the local compliance due to the contact stresses.

Fig. 1 — A Simple Spur Gear System.

Fig. 2 — A Mathematical Model of the Transmission System.

Fig. 3 — Element Modelling of a Gear Tooth.

To determine q_j let the tooth be divided into elements as shown in Fig. 3. Let i be a typical element with thickness T_i, cross section area A_i, and second moment of inertia I_i. Let L_{ij} be the distance between element i and point j along the x-axis. Let β_j be the angle between W_j and the y-axis. (See Fig. 3.)

Consider the tooth to be a nonuniform cantilever beam. Let q_{bj} be the contribution to q_j by the bending, shear, and axial deforma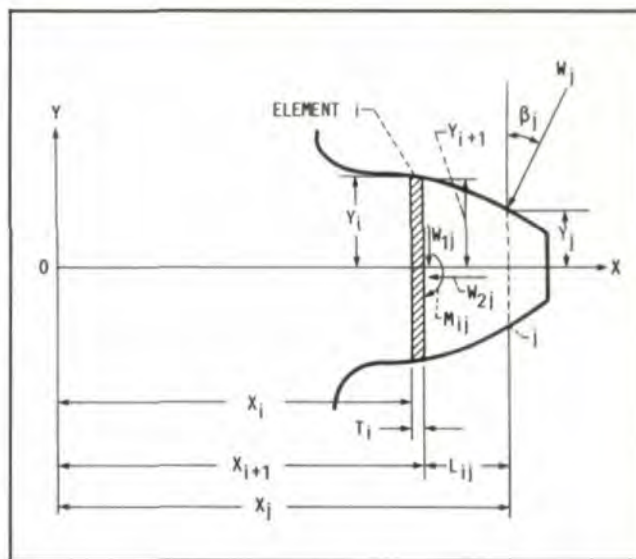tion of the tooth. The q_{bj} may be represented as the sum of the deformation in the elements i beneath point j. That is,

$$q_{bj} = \sum_{i=1}^{n} q_{bij} \tag{6}$$

where n is the number of elements beneath j and q_{bij} is the deformation of element i due to the load W_j.

KLINGELNBERG

Puts it all together with exciting, new products to keep you competitive!

Gearmakers worldwide face customer demands for highest quality and on-time delivery at fiercely competitive prices. Meeting these demands requires greater flexibility, productivity and the ability to integrate new technology. Recognizing your ultimate goals – customer satisfaction and profitability – Klingelnberg global technology is ready with the most advanced CNC Spiral Bevel Gear Generators and Grinders, and the most complete line of CNC Gear Checkers available... anywhere.

We've put it all together:

Spiral Bevel Gear Applications

- KNC 40/60 fully CNC controlled Generators
- AMK Large Gear Generators
- W800CNC (Wiener System) Grinder
- CNC Inspection Equipment
- Quench Presses

Worm and Rotor Grinding Applications

- HNC Series of CNC controlled Grinders
- CNC Inspection Systems

Parallel Axis Gear Applications

- CNC controlled gear Inspection Systems
- SNC Series of CNC Hob Sharpeners
- Gear Cutting Tool Inspection Systems
- Hurth Product Line: CNC Shavers, Hard & Fine Finishers, Shaving Cutter Grinders and Deburring/Chamfering Equipment.

GEARMAKING!

The KNC-40/60 Gear Generators

These new, fully CNC, 8 axis gear generators produce Spiral Bevel Gears up to 24" O.D. Perfect for small batch or intermediate level production runs, the KNC Series generates Spiral Bevel Gears of any geometry by continuous or single indexing operation. Its program storage capacity for 250 different workpieces and unlimited storage capacity with a DNC interface, makes it the most flexible gear generator you can buy.

The W800CNC Gear Grinder (Wiener System)

With leading edge technology, the W800CNC becomes the universal Spiral Bevel Gear grinder for any gear geometry. Perfect for ground gear quality applications up to 31.5" O.D., the grinder offers great versatility, short set-ups and superior accuracy.

The PNC Series Gear Checkers

Compact, new CNC controlled gear checkers provide fully automatic measuring of gears up to 80" O.D. Fast operation, high accuracy, excellent documentation and a wide variety of software modules, form the perfect gear checking package.

For the latest information on Klingelnberg systems that satisfy customer demands, for increased productivity and profitability, contact our representative. Or, write to Klingelnberg Gear Technology Inc., 15200 Foltz Industrial Parkway, Strongsville, OH 44136 Phone: 216/572-2100; FAX: 216/572-0985.
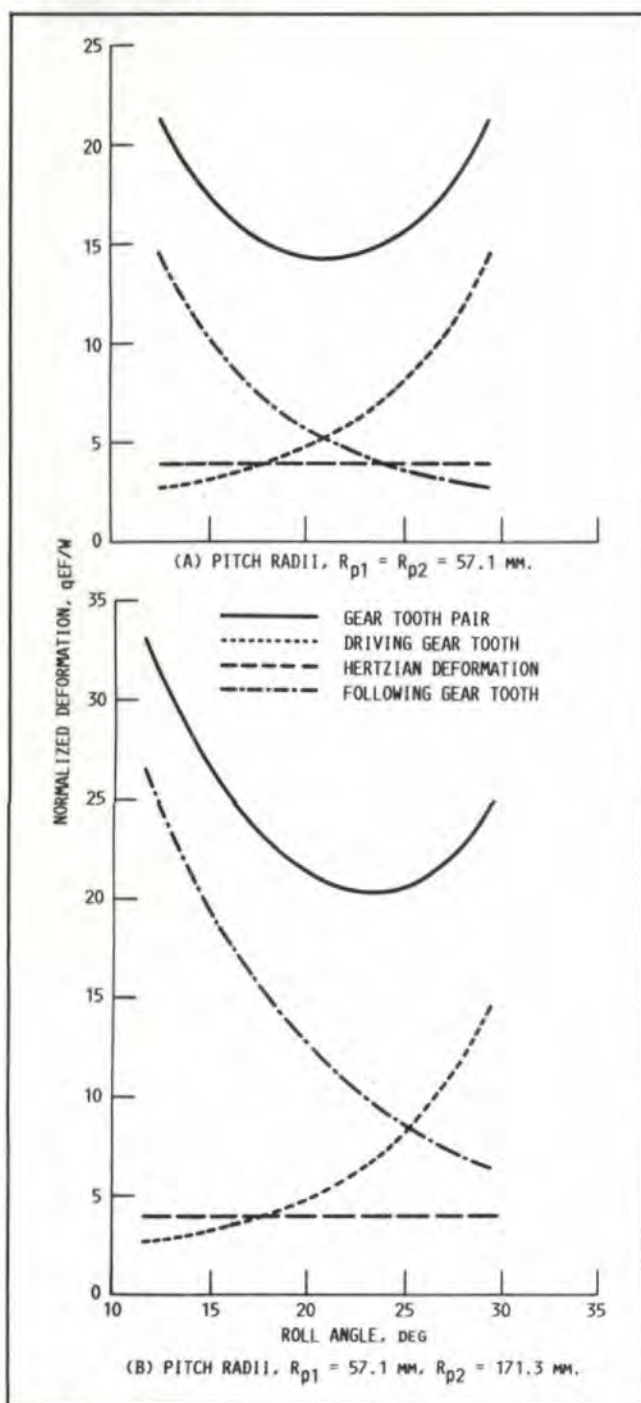
KLINGELNBERG

...Puts it all together.

Fig. 4—Normalized Deformation of a Pair of Teeth. Module, 3.18 mm; Pressure Angle, 20°; Face Width, F = 25.4 mm; Modulus of Elasticity, E = 207 GPa; Applied Load, W = 105 KN/m.

With standard analysis q_{bij} is found to have the value:[8, 14, 15]

$$q_{bij} = (W_j/E_e)\left\{ \cos^2\beta_j\left[\left(T_i^3 + 3T_i^2L_{ij} + 3T_iL_{ij}^2\right)\middle/3I_i\right]\right.$$

$$- \cos\beta_j\sin\beta_j\left[\left(T_i^2Y_j + 2T_iY_jL_{ij}\right)\middle/2I_i\right]$$

$$\left. + \cos^2\beta_j[12(1 + \nu)T_i/5A_i] + \sin^2\beta_j(T_i/A_i)\right\} \quad (7)$$

where Y_j is the half-tooth thickness at element i (See Fig 3.), ν is Poisson's ratio, and E_e is the "effective elastic modulus" depending upon whether the tooth is wide (plane strain) or narrow (plane stress). Specifically, for a "wide" tooth, where the ratio of the width to thickness at the pitch point exceeds 5,[14] E_e is

$$E_e = \frac{E}{(1 - \nu^2)} \quad (8)$$

where E is Young's modulus of elasticity. For a "narrow" tooth (width-to-thickness ratio less than 5), E_e is

$$E_e = E \quad (9)$$

Expressions similar to Equation 7 hold for q_{fj}, the contribution to q_j for the deformation due to the flexibility of the tooth fillet and foundation.[15]

Let q_{cj} be the contribution to q_j from the local compliance due to contact stresses. With the procedures of Lundberg and Palmgren[16] q_{cj} may be expressed as

$$q_{cj} = \frac{1.275}{E^{0.9}F^{0.8}W_j^{0.1}} \quad (10)$$

where F is the width of the tooth.

Hence, by superposition, the deformation at j in the direction of W_j is

$$q_j = q_{bj} + q_{fj} + q_{cj} \quad (11)$$

The above expressions were used to calculate the deformations for two different gear pairs. The results are shown graphically in Figs. 4a and b.

Shaft stiffness. — The shaft stiffness K_s is given by the standard expression

$$K_s = \frac{JG}{l} \quad (12)$$

where G is the shear modulus, l is the shaft length, and J is the polar moment of area given by

$$J = \frac{\pi D^4}{32} \quad (13)$$

where D is the shaft diameter.

DAMPING

Shaft damping. — Next consider the damping coefficients C_{s1}, C_{s2}, and C_g. Damping in the shafts is due to the shaft material. In Equations 1 to 4 the coefficients C_{s1} and C_{s2} are taken to have the form

$$C_{s1} = 2\xi_s\left\{ \frac{K_{s1}}{\frac{1}{J_M} + \frac{1}{J_1}} \right\}^{1/2} \quad (14)$$

(A) BUCKINGHAM'S MODEL.

(B) BENEDICT AND KELLEY'S MODEL.
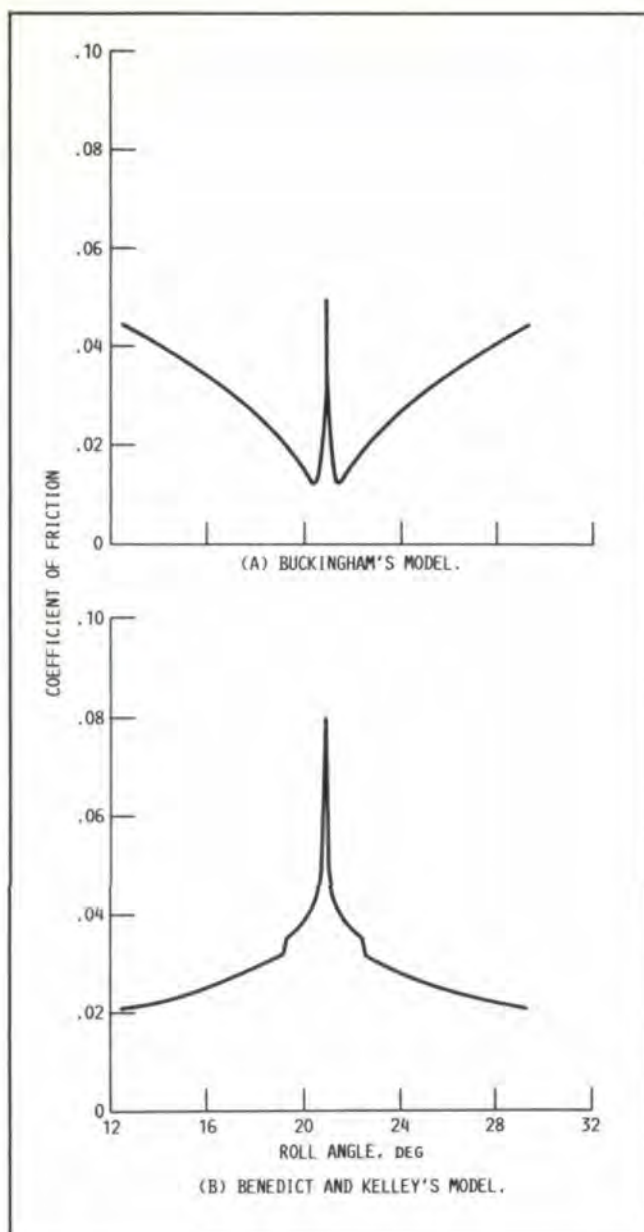
ROLL ANGLE, DEG

COEFFICIENT OF FRICTION

Fig. 5 – Friction Coefficient of Gears in Figure 4a at 1500 RPM.

and

$$C_{s2} = 2\xi_s \left\{ \frac{K_{s2}}{\dfrac{1}{J_L} + \dfrac{1}{J_2}} \right\}^{1/2} \qquad (15)$$

where ξ_s represents the damping ratio. Experiments have shown that ξ_s has values between 0.005 and 0.075.[17]

Mesh damping. — Similarly, the effect of damping of the gear mesh is taken as

$$C_g = 2\xi \left[\frac{K_g R_{b1}^2 R_{b2}^2 J_1 J_2}{R_{b1}^2 J_1 + R_{b2}^2 J_2} \right]^{1/2} \qquad (16)$$

where, as before, ξ is the damping ratio. Measurements have shown ξ to have values between 0.03 and 0.17.[9-10]

Friction. — Equations 1 to 4 contain terms T_{f1} and T_{f2} which represent the frictional moments of the driving and driven gears. These moments occur because of the relative sliding of the gear teeth. Buckingham[18] has recorded a

semiempirical formula for the friction coefficient f of boundary lubrication as

$$f = 0.05e^{-0.125V_{sl}} + 0.002\sqrt{V_{sl}} \qquad (17)$$

where V_{sl} is the sliding speed measured in in./sec. An analogous expression for elastohydrodynamic lubrication has been developed by Benedict and Kelley[19] and by Anderson and Loewenthal[20] as follows:

$$f = 0.0127 \log (C_i W / F\mu_o V_{sl} V_R^2) \qquad (18)$$

where

C_i = 29.66 (SI units)
= 45.94 (English units)
W = the applied load, N/m (lb/in.)
F = face width, mm (in.)
V_R = rolling velocity, mm/sec (in./sec)
μ_o = lubricant viscosity, N-sec/m^2 (lb-sec/in.^{2})

Figures 5a and b show graphs of the friction coefficient as given by Equations 17 and 18 as a function of the roll angle. Figs. 6a and b show the resulting effect upon the friction torque.

MESH ANALYSIS

Fig. 7 illustrates the motion of a pair of meshing teeth. The initial contact occurs at A, where the addendum circle of the driven gear intersects the line of action. As the gears rotate the point of contact will move along the line of action APD.

Nomenclature

A_i	cross section area of ith element of gear teeth, mm^2 (in.^{2})	R_p	pitch radii of gears, mm
C_g	damping coefficient, gear tooth mesh, N-sec (1b-sec)	t_i	thickness of element i, mm
C_s	damping coefficient of shaft, N-m-sec (in.-lb-sec)	T_L	torque on load, N-m
E_e	effective modulus of elasticity, N/m^2 (lb./in^2)	T_M	torque on motor, N-m
F	*tooth face width, mm (in.)*	T_{f1}	*torque on gear 1, N-m*
G	shear modulus, N/m^2 (lb/in.^{2})	T_{f2}	torque on gear 2, N-m
I_i	second moment of inertia of ith element of gear teeth, mm^2 (in.^{2})	V_{s1}	sliding velocity during tooth mesh, mm/sec
		V_R	rolling velocity, mm/sec
J_L	polar moment of inertia of load, m^2-Kg	W	applied load, N/m (lb/in.)
J_M	polar moment of inertia of motor, m^2-Kg	x_i	x-coordinate of element i, mm (in.)
J_1	polar moment of inertia of gear 1, m^2-Kg	y_i	y-coordinate of element i, mm (in.)
J_2	polar moment of inertia of gear 2, m^2-Kg	β	load angle, rad
K_g	stiffness of gear tooth, Nm/rad-m	δ	backlash, mm (in.)
K_s	stiffness of shaft, N-m/rad	θ	angular displacment, rad
L_{ij}	distance between elements i and j, mm	$\dot{\theta}$	angular velocity, rad/sec
q_b	gear tooth deformation due to beam deflection, mm	$\ddot{\theta}$	angular acceleration, rad/sec^2
q_c	gear tooth deformation due to contact deformation, mm	μ_o	lubricant viscosity, N-sec/m^2 (lb-sec/in.^{2})
q_f	gear tooth deformation due to foundation flexibility, mm	ν	Poisson's ratio
$q=q_b+q_f+q_c$ total gear tooth deformation, mm (in.)		ξ	damping ratio
R_b	base radii of gears, mm (in.)		

(A) BUCKINGHAM'S MODEL.

TORQUE, N·M

(B) BENEDICT AND KELLEY'S MODEL.

Fig. 6 – Friction Torque Variation Along the Contact Path for Gears in Figure 4a at 1500 RPM.

Fig. 7 – Illustration of Gear Meshing Action.

Fig. 8 – Typical Stiffness and Load Sharing of Low Contact Ratio Gears of Figure 4a.

When the tooth pair reaches B, the recessing tooth pair disengages at D leaving only one zone. When the tooth pair reaches point C, the next tooth pair begins engagement at A and starts another cycle.

In the analysis, the position of the contact point of the gear teeth along the line of action is expressed in terms of roll angles of the driving gear tooth.

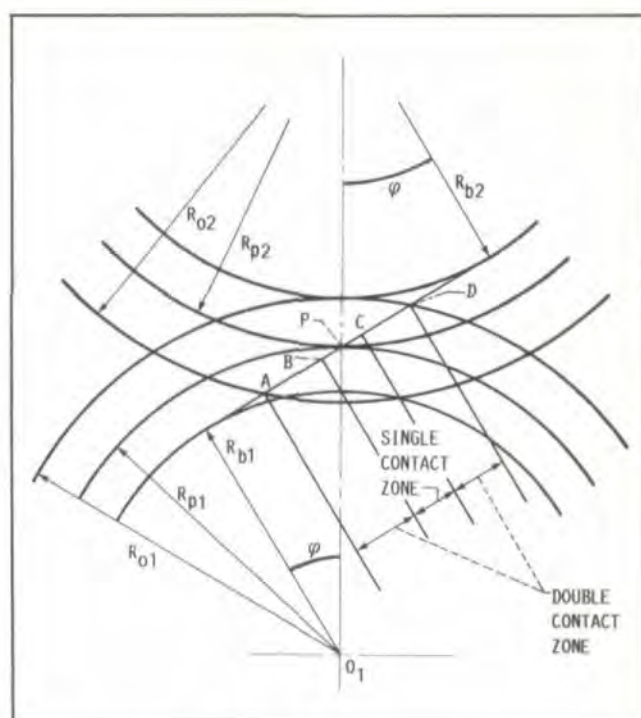Fig. 8 shows typical stiffness and load sharing character-istics through a mesh cycle. Let a series of mating tooth pairs be denoted as a, b, c, d and let points A, B, P, C, D be the same as those in Fig. 7. Then AB and CD represent the dou-ble contact regions, BC represents the single contact region, and, as before, P is the pitch point.

The stiffness values at double contact regions are clearly much higher than those at single contact regions. When gears rotate at appreciable speed, this time-varying stiffness

as shown in Fig. 8 is the major excitation source for the dynamic response of the system.

Discussion

The objective of this analysis is to establish the governing differential equations and to present a procedure for solution. As noted, the equations themselves are nonlinear. However, they may be efficiently solved by using the following linearized-iterative procedure.

The linearized equations may be obtained by dividing the mesh cycle into n equal intervals. Let a constant input torque T_M be assumed. Let the output torque T_L be fluctuating because of damping in the gear mesh, because of friction, and because of time-varying mesh stiffness.

Let initial values of the angular displacements be obtained by preloading the input shaft with the nominal torque carried by the system. Initial values of the angular speeds may be taken from the nominal operating speed of the system.

The iterative process is then as follows: the calculated values of the angular displacements and angular speeds after one period are compared with the assumed initial values. Unless the differences between them are sufficiently small, the procedure is repeated by using the average of the initial and calculated values as new initial values.

Finally, observe that the term $(R_{b1}\theta_1 - R_{b2}\theta_2)$ in the equation of motion represents the relative dynamic displacement of the gears. Let δ represent the backlash. Let gear 1 be the driving gear. The following conditions can occur:

Case 1

The normal operating case is

$$R_{b1}\theta_1 - R_{b2}\theta_2 > 0 \qquad (19)$$

The dynamic mesh force F is then

$$F = K_g(t) R_{b1}\theta_1 - R_{b2}\theta_2) + C_g(t)(R_{b1}\dot{\theta}_1 - R_{b2}\dot{\theta}_2) \qquad (20)$$

Case 2

$$R_{b1}\theta_1 - R_{b2}\theta_2 \lesseqgtr 0 \text{ and } |R_{b1}\theta_1 - R_{b2}\theta_2| \lesseqgtr \delta \qquad (21)$$

In this case, the gears will separate and the contact between the gears will be lost. Hence,

$$F = 0 \qquad (22)$$

Case 3

$$R_{b1}\theta_1 - R_{b2}\theta_2 < 0 \text{ and } |R_{b1}\theta_1 - R_{b2}\theta_2| > \delta \qquad (23)$$

In this case, gear 2 will collide with gear 1 on the backside. Then,

$$F = K_g(t)[(R_{b2}\theta_2 - R_{b1}\theta_1) - \delta] + C_g(t) (R_{b1}\dot{\theta}_1 - R_{b2}\dot{\theta}_2) \quad (24)$$

Conclusion

A low contact ratio spur gear transmisson model is devleoped. The model includes inertias of load and power source, stiffness of shaft, time-varying mesh stiffness, and damping and friction inside gear transmissions.

Governing equations of the model are derived and a linearized iterative procedure for the solution is presented.

Parameter study including rotating speed, diametral pitch, applied load, damping, stiffness, and inertia will be presented in Part 2 of this article.

References

1. LEWIS, W. "Investigations of the Strength of Gear Teeth." *Proceedings of the Engineers Club of Philadelphia*, 1893, pp. 16-23.

2. BUCKINGHAM, E. *Dynamic Loads on Gear Teeth*. ASME Research Publication, New York, 1931.

3. ATTIA, A.Y. "Dynamic Loading of Spur Gear Teeth." *J. Eng. Ind.*, Vol. 81, No. 1, Feb. 1959, pp. 1-9.

4. NIEMANN, G. & RETTIG, H. "Error-Induced Dynamic Gear Tooth Loads." *Proceedings of the International Conference on Gearing*, 1958, pp. 31-42.

5. HARRIS, S.L. "Dynamic Loads on the Teeth of Spur Gears." *Proc. Inst. Mech. Eng.*, Vol. 172, 1958, pp. 87-112.

6. SEIREG, A. & HOUSER, D.R. "Evaluation of Dynamic Factors for Spur and Helical Gears." *J. Eng. Ind.*, Vol. 92, No. 2, May 1970, pp. 504-515.

7. ICHIMARU, K. & HIRANO, F. "Dynamic Behavior of Heavy-Loaded Spur Gears." *J. Eng. Ind.*, Vol. 96, No. 2, May 1974, pp. 373-381.

8. CORNELL, R.W. & WESTERVELT, W.W. "Dynamic Tooth Loads and Stressing for High Contact Ratio Spur Gears." *J. Mech. Des.*, Vol. 100, No. 1, Jan. 1978, pp. 69-76.

9. KASUBA, R. & EVANS, J.W. "An Extended Model for Determining Dynamic Loads in Spur Gearing." *J. Mech. Des.*, Vol. 103, No. 2, Apr. 1981, pp. 398-409.

10. WANG, K. L. & CHENG, H.S. "A Numerical Solution to the Dynamic Load, Film Thickness, and Surface Temperatures in Spur Gears, Part 1 — Analysis." *J. Mech. Des.*, Vol. 103, No. 1, Jan. 1981, pp. 177-187.

11. LEWICKI, D.G. "Predicted Effect of Dynamic Load on Pitting Fatigue Life for Low-Contact-Ratio Spur Gears." NASA TP-2610, 1986.

12. NAGAYA, K. & UEMATSU, S. "Effects of Moving Speeds of Dynamic Loads on the Deflections of Gear Teeth." *J. Mech. Des.*, Vol. 103, No. 2, Apr. 1981, pp. 357-363.

13. TERAUCHI, Y., NADANO, H. & NOHARA, M. "On the Effect of the Tooth Profile Modification on the Dynamic Load and the Sound Level of the Spur Gear." *Bull. JSME*, Vol. 25, No. 207, Sept. 1982, pp. 1474-1481.

14. CORNELL, R.W. "Compliance and Stress Sensitivity of Spur Gear Teeth." *J. Mech. Des.*, Vol. 103, No. 2, Apr. 1981, pp. 447-459.

15. LIN, H.H. & HUSTON, R.L. "Dynamic Loading on Parallel Shaft Gears." (UC-MIE-051586-19, University of Cincinnati; NASA Grant NSG-3188) NASA CR-179473, 1986.

16. LUNDBERG, G. & PALMGREN, A. "Dynamic Capacity of Rolling Bearings." *Acta Polytech. Mech. Eng. Sci.*, Vol. 1, No., 3, 1947.

17. HAHN, W.F. "Study of Instantaneous Load to Which Gear Teeth are Subjected." Ph.D. Thesis, University of Illinois, 1969.

18. BUCKINGHAM, E. *Analytical Mechanics of Gears*. Dover, 1949.

19. BENEDICT, G.H. & KELLEY W.W. "Instantaneous Coefficients of Gear Tooth Friction." *ASLE Trans.*, Vol. 4, No. 1. Apr. 1961, pp. 59-70.

20. ANDERSON, N.E. & LOEWENTHAL S.H. "Spur Gear System Efficiency at Part and Full Load." NASA TP-1622, 1980.